Glial activation in the collagenase model of nociception associated with osteoarthritis

Sara Adães[1,2,3], Lígia Almeida[1,2,3], Catarina S Potes[1,2,3], Ana Rita Ferreira[1], José M Castro-Lopes[1,2,3], Joana Ferreira-Gomes[1,2,3] and Fani L Neto[1,2,3]

Abstract

Background: Experimental osteoarthritis entails neuropathic-like changes in dorsal root ganglia (DRG) neurons. Since glial activation has emerged as a key player in nociception, being reported in numerous models of neuropathic pain, we aimed at evaluating if glial cell activation may also occur in the DRG and spinal cord of rats with osteoarthritis induced by intra-articular injection of collagenase.

Methods: Osteoarthritis was induced by two injections, separated by three days, of 500 U of type II collagenase into the knee joint of rats. Movement-induced nociception was evaluated by the Knee-Bend and CatWalk tests during the following six weeks. Glial fibrillary acidic protein (GFAP) expression in satellite glial cells of the DRG was assessed by immunofluor-escence and Western Blot analysis; the pattern of GFAP and activating transcription factor-3 (ATF-3) expression was also compared through double immunofluorescence analysis. GFAP expression in astrocytes and IBA-1 expression in microglia of the L3–L5 spinal cord segments was assessed by immunohistochemistry and Western Blot analysis. The effect of the intrathecal administration of fluorocitrate, an inhibitor of glial activation, on movement-induced nociception was evaluated six weeks after the first collagenase injection.

Results: GFAP expression in satellite glial cells of collagenase-injected animals was significantly increased six weeks after osteoarthritis induction. Double immunofluorescence showed GFAP upregulation in satellite glial cells surrounding ATF-3-positive neurons. In the spinal cord of collagenase-injected animals, an ipsilateral upregulation of GFAP and IBA-1 was also observed. The inhibition of glial activation with fluorocitrate decreased movement- and loading-induced nociception.

Conclusion: Collagenase-induced knee osteoarthritis leads to the development of nociception associated with movement of the affected joint and to the activation of glial cells in both the DRG and the spinal cord. Inhibition of glial cell activation by fluorocitrate decreases these osteoarthritis-associated nociceptive behaviours. These results suggest that glial cell activation may play a role in the development of chronic pain in this experimental model of osteoarthritis.

Introduction

Pain associated with osteoarthritis (OA) is yet to be fully understood. Recent studies have been pointing towards the possibility of a neuropathic component in OA-associated nociception.[1–4] Recently, our group has shown that OA progression leads to the expression of neuronal injury markers in the dorsal root ganglia (DRG), both in collagenase-[1] and monoiodoacetate (MIA)-induced OA.[2] Using the collagenase model,

[1]Instituto de Investigação e Inovação em Saúde, Universidade do Porto, Porto, Portugal
[2]Morphysiology of the Somatosensory System Group, Instituto de Biologia Molecular e Celular, Porto, Portugal
[3]Departamento de Biologia Experimental, Faculdade de Medicina da Universidade do Porto, Porto, Portugal

Corresponding author:
Sara Adães, Departamento de Biologia Experimental, Faculdade de Medicina da Universidade do Porto, Alameda Prof Hernâni Monteiro, 4200-319 Porto, Portugal.
Email: sadaes@med.up.pt

we also demonstrated that, although inflammation may contribute to nociceptive behaviours at the onset of OA, neuropathic-like changes become preponderant as disease progresses. This is highlighted by the inefficacy of non-steroidal anti-inflammatory drugs at late time points, in contrast to the efficacy of gabapentin when experimental OA is fully developed.[1,5]

The neuropathic-like features in OA pain may arise from injury of nerve endings in the subchondral bone, which becomes exposed as disease progresses.[1,2,5] Peripheral nerve injury (PNI) is known to activate both neurons and glia of the peripheral nervous system (PNS) and central nervous system (CNS).[6–9] In the PNS, satellite glial cells (SGCs) that tightly surround neurons in the DRG[10] are activated following PNI, contributing to the maintenance of neuropathic pain.[11–13] This activation is characterized, among others, by cell proliferation and hypertrophy, increased number of gap junctions and cell coupling, and altered production of various molecules, including an upregulation of glial fibrillary acidic protein (GFAP) expression.[11,14,15] GFAP is present at low levels in non-activated SGCs,[12] but it is over-expressed in SGCs in different models of PNI,[12,16–20] being a marker of their activation.[21,22] In the CNS, glial cells also participate in normal and pathological processes[23–26]; there is strong evidence that the activation of both microglia and astrocytes is implicated in the induction and maintenance of neuropathic pain by mediating important neuron-glia cross-talk mechanisms.[6–9] Several studies have shown that the selective inhibition of these glial cells' metabolism attenuates the nociceptive behaviour in various pain models.[12,27] One of the drugs currently used is fluorocitrate, which selectively inhibits the tricarboxylic acid cycle in SGCs, astrocytes and microglia by blocking aconitase, a glia-specific metabolic enzyme,[28,29] and that has been shown to effectively reduce mechanical allodynia in animal models of neuropathic pain.[12]

In this study, we hypothesized that, after six weeks of collagenase-induced OA development, when the neuropathic component of nociception is prominent, glia activation may also contribute to the mechanisms of nociception. To test this hypothesis, we assessed the activation of SGCs in the DRG of OA animals through the expression of GFAP, and we evaluated whether there is a link between PNI and SGC activation by performing a double immunofluorescence analysis of the expression of the neuronal injury marker activating transcription factor (ATF)-3 in neurons[30] and of GFAP in their enveloping SGCs. We also assessed the activation of astrocytes and microglia in the spinal cord (SC) through the expression of GFAP[7] and IBA-1,[31] respectively. Finally, we tested the effect of the intrathecal administration of fluorocitrate on movement- and loading-induced nociceptive behaviour in the collagenase-induced OA animals. With these

experiments, we aimed at determining if, at six weeks of OA progression, when neuropathy correlates with nociception,[1] there is also glial cell activation in the DRG and SC, as seen in models of neuropathic pain, and if their inactivation can decrease the nociceptive behaviour.

Material and methods

Animals

Adult male Wistar rats (230 ± 30 g, Charles River, France) were housed with water and food ad libitum, at a constant temperature of $22°$C and controlled lighting (12 h light/12 h dark cycle). Experimental procedures were performed in accordance with the ethical guidelines for the study of experimental pain in conscious animals,[32] and the European Council Directive 2010/63/EU, and were approved by the Ethical Committee for Health of Centro Hospitalar de São João, Porto, Portugal.

Osteoarthritis induction

Intra-articular (i.a.) injections were performed using a Hamilton syringe with a 26-G needle inserted through the patellar ligament into the left knee joint cavity of animals briefly anesthetized with isoflurane (5% for induction, 2% for maintenance). Animals received two 25-μL injections, one on day 0 and another on day 3, of either sterile saline (control group) or 500 U of type II collagenase from *Clostridium histolyticum* (Sigma-Aldrich) dissolved in saline and filtered through a 0.22-μm membrane.[5,33] Animals were randomly assigned to each group before the first injection.

Nociceptive behaviour

A total of 37 rats injected with saline or collagenase were divided in three experimental groups. One group was used for immunohistochemical analysis (11 animals; $n = 5$ for saline, $n = 6$ for collagenase) and was euthanized six weeks after the first injection; the nociceptive behavioural data for this group were previously presented.[1] The second group was used for Western Blot (WB) analysis (16 rats; $n = 8$ for saline, $n = 8$ for collagenase) and was euthanized after six weeks; the nociceptive behavioural data of this group are presented here. The third group was used for the inhibition of glial activation with fluorocitrate at the sixth week of OA progression (10 collagenase-injected rats) and was then euthanized. Movement- and loading-induced nociception was evaluated in all animals by the Knee-Bend and CatWalk tests as previously described.[5,34] Briefly, for the Knee-Bend test, the squeaks and/or struggle reactions in response

to five alternate flexions and extensions of the knee joint were scored. The contralateral knee was always tested first, as to avoid increased contralateral scores due to manipulation of the injected knee. Results were presented as the difference between the ipsilateral and the contralateral Knee-Bend score. For the CatWalk test, animals were placed in a platform where a bright image of the paw print was produced. The signal intensity depended on the area of the paw in contact with the platform and the pressure applied. For each hind paw, the total paw print intensity (mean pixel intensity × number of pixels) was determined, allowing the comparison of the area/pressure applied by each paw. Results were expressed as the percentage of the total ipsilateral paw print intensity (%TIPPI) in the sum of both paw prints. The CatWalk test was always performed prior to the Knee-Bend to minimize the effect of manipulating the affected knee on the animals' gait. Testing was performed blindly, always by the same experimenter who did not participate in the assignment of the animals to each group. Animals were tested on day 0 and weekly after injection, until each group's endpoint. For the Knee-Bend test, results are presented as the difference between the ipsilateral and the contralateral Knee-Bend score. For the CatWalk test, results are expressed as the percentage of the total ipsilateral paw print intensity (%TIPPI) in the total intensity of both paw prints. The CatWalk test was always performed prior to the Knee-Bend test to minimize the effect of manipulation of the affected knee joint on the animals' gait.

Tissue processing

For the immunohistochemistry group, animals were perfused with 4% paraformaldehyde six weeks after the first injection of saline or collagenase. Their ipsilateral L3, L4 and L5 DRG and the L3–L5 SC segments were dissected, post-fixed in the same fixative (4 h) and kept in 30% sucrose with 0.01% sodium azide. DRG were serially sliced in 12 μm sections using a cryostat, with every tenth section collected in the same slide. Each DRG was always cut longitudinally yielding 8–10 sections per slide, on average. SC segments were serially sliced in 40 -μm free-floating transverse sections using a freezing microtome. The contralateral side was identified with a small cut in the ventral horn before sectioning. Sections were then stored at −20°C in a cryoprotective solution until further processing.[35]

Immunohistochemistry

Immunofluorescence reactions in the DRG were performed in slides containing every tenth section of ipsilateral L3, L4 or L5 DRG of rats sacrificed six weeks after collagenase or saline injection, as previously described.[5,36] DRG sections were incubated with either rabbit anti-GFAP (1:1000, Abcam) or mouse anti-ATF-3 (1:200, Abcam), overnight at room temperature. Secondary detection was performed with either Alexa Fluor-568 donkey anti-rabbit or Alexa Fluor-488 donkey anti-mouse secondary antibodies (1:1000, 1 h, room temperature, Molecular Probes). Slides were mounted with glycerol. Negative controls were performed without the primary antibody. Images were acquired in a fluorescence microscope (Axio Imager.Z1), through an AxioCam MRm digital camera with AxioVision 4.6 software (Carl Zeiss MicroImaging GmbH). For GFAP labelling, all neurons having at least half of its circumference surrounded by GFAP-labelled SGCs were considered GFAP-encircled neurons,[12,36] and were counted. This number was divided by the total number of neurons counted in the analysed sections. Results are presented as the percentage of GFAP-encircled neurons in L3, L4 and L5 DRG. For ATF-3, the total number of neurons and the number of labelled neurons were counted. Data are presented as the percentage of neurons expressing ATF-3 in L3, L4 and L5 DRG. Double labelling for ATF-3 and GFAP was performed by simultaneous reaction for both antibodies and quantified as described.

Immunohistochemistry for GFAP and IBA-1 in the SC was performed as previously described.[37] Briefly, the endogenous peroxidase activity was inhibited with phosphate-buffered saline (PBS) containing 0.3% hydrogen peroxide for 30 min, and sections were then incubated for 1 h in a blocking solution (glycine 0.15 M and 10% normal swine serum). Immunodetection was performed with either rabbit anti-GFAP (1:2500, overnight RT, Abcam) or rabbit anti-IBA-1 (1:2000, overnight RT, Wako). For secondary detection, sections were incubated for 1 h in biotinylated swine anti-rabbit antiserum (1:200, Dako) and for another hour in avidin–biotin complex (ABC) conjugated with horseradish peroxidase (1:200, Vector Labs). Visualization of the immunostaining was achieved using the 3,3'-diaminobenzidine tetrahydrochloride (DAB) reaction (5 min in 0.05 M Tris buffer containing 0.05% DAB and 0.003% hydrogen peroxide). Sections were mounted on gelatine-coated slides, cleared in xylene and coverslipped with Eukitt (Sigma Aldrich).

Labelling was quantified in random sections from the L3, L4 and L5 segments of the SC (6 sections per segment). Images were captured with a light microscope (Axioskop 40) coupled with an AxioCam MRc5 digital camera and Axiovision 4.6 image software (Carl Zeiss MicroImaging GmbH). The acquisition conditions such as amplification of the objective, light intensity, contrast and hue were maintained constant. Immunoreactivity was quantified by densitometry in the ipsilateral and contralateral dorsal horn using

Image J. Laminae I–III were delimited taking as reference the Rat Brain Atlas of Paxinos and Watson,[38] and the same area was used in the ipsilateral and contralateral sides. Results are presented as the ipsilateral/contralateral ratio.

Western Blot

WB experiments were performed to evaluate the expression of GFAP in the DRG, and the expression of both GFAP and IBA-1 in the SC of control and collagenase injected rats, six weeks after the first injection. Animals were euthanized by decapitation under pentobarbital anaesthesia and samples were extracted from freshly harvested L3–L5 ipsilateral and contralateral DRGs and SC segments. For each animal, the L3–L5 SC segments or DRG were pooled separately for the ipsilateral and contralateral sides, and were then lysed in radio immunoprecipitation assay (RIPA) buffer (Sigma Aldrich) containing cocktails of protease and phosphatase inhibitors (1:100, Sigma-Aldrich P8340, P5726 and P0044). The samples were centrifuged (20 minutes at 20,000 g), the pellets were discarded and the supernatants were used for analysis. The proteins were quantified by the bicinchoninic acid protein assay. After heating at $94°C$, 20 mg of protein were loaded in each lane and separated on 12.5% sodium dodecyl sulphate-polyacrylamide (SDS/PAGE) gels. The proteins were then transferred into nitrocellulose membranes which were blocked with non-fat milk (5% milk powder diluted in Tris buffer saline tween20; TBST buffer) for 1 h, at room temperature, to prevent non-specific bindings. Immunodetection was performed by overnight incubation at $4°C$ with mouse anti-GFAP (1:5000, 51 kDa, Millipore) or rabbit anti-IBA-1 (1:500, 17 kDa, Wako). Rabbit anti-glyceraldehyde 3-phosphate dehydrogenase (GAPDH, 1:5000, 37 kDa, Abcam) was used as a loading control. Secondary detection was performed by incubation with goat anti-mouse secondary antibody conjugated with horseradish peroxidase (HRP, Santa Cruz Biotechnology, Inc) or donkey anti-rabbit secondary antibody conjugated with HRP (Jackson Laboratories), diluted 1:5000 in TBST with 5% milk powder, for 1 h at room temperature. Antibody binding was visualized with the SuperSignal West Pico Chemiluminescent Substrat kit (Thermo Scientific), and the bands were detected using a ChemiDoc MP System 170-8280 (Bio-Rad). Each blot, containing independent samples, was run in duplicates, and means were used as raw values. Band intensity was determined by densitometric analysis of the signal intensity in the blots using Image J. Both the areas of the lanes and the background signal were used for normalization. The ratio between GFAP or IBA-1 and GAPDH protein levels was calculated for each sample. Additionally, ratios between the ipsilateral and contralateral levels were calculated in control and collagenase-injected animals.

Inhibition of glial activation

The effect of a single administration of the glial activation inhibitor fluorocitrate in the behavioural responses of OA animals was evaluated in a different experimental group. At six weeks after collagenase injection, fluorocitrate (Sigma-Aldrich) was administered intrathecally in order to reach the lumbar spinal segments ($n = 5$, 30 μL, 0.1 nM dissolved in PBS 0.01 M with 0.3% HCl 2 M; pH 6.0^{39}) according to a protocol adapted from Ossipov et al.[40] and De la Calle et al.[41] Briefly, rats were anesthetized with isoflurane (5% for induction, 2% for maintenance), the lower half of the animal's back was shaved and disinfected. Using the anterior part of the iliac crest as a tactile landmark for the L6 vertebra, a 2-cm longitudinal incision was made with a scalpel and the fascia of the paravertebral muscles was separated to the sides with the help of cotton plugs. Animals were injected either at the L5–L6 or L6–S1 intervertebral space using a 26-gauge needle connected to a 100-μL Hamilton syringe by introducing the needle through the widest intervertebral space, lowering it until contact with the vertebral body and penetrating into the intrathecal space perceived by a change of resistance. Correct dura puncture and position of the tip of the needle was verified by a reflexive flick of the tail or a hind paw flinch. Behaviour was assessed by the Knee-Bend and CatWalk tests at 1, 2, 3, 4 and 6 h after administration, as determined in preliminary experiments. Baseline values of nociception were determined before drug administration ($t = 0$ h). Control animals ($n = 5$) received an intrathecal administration of vehicle, also six weeks after collagenase injection, and behavioural assessment was performed at the same time points.

Statistical analysis

Results are presented as mean $\pm$ SEM. The normality of all data was assessed by the Kolmogorov–Smirnov test. Behavioural data for movement induced-nociception in control and collagenase-injected groups was analysed by two-way analysis of variance (ANOVA), for factors time and group, followed by Bonferroni post-hoc test for multiple comparisons between groups. The Mann–Whitney test was used for the immunofluorescence and WB data. The pharmacological data were analysed by repeated measures ANOVA followed by Dunnett's post-hoc test. In all statistical analysis, a level of significance of $p < 0.05$ was assumed.

Results

Movement-induced nociception

The Knee-Bend (Figure 1(a)) and CatWalk (Figure 1(b)) tests were used to evaluate movement-induced nociception following the i.a. injection of saline or collagenase. In both tests, saline-injected control animals showed, at all time points, behavioural responses similar to those observed prior to the injection. In collagenase-injected animals, the more pronounced changes were observed one week after the first collagenase injection (Figure 1(a) and (b)). Knee-Bend scores (Figure 1(a)) increased from 0.1 ± 0.1 on day 0 to 11.3 ± 0.9 at week 1 ($p < 0.001$) and remained significantly higher than those observed in control animals during the whole experimental period (9.4 ± 1.3, $p < 0.001$). In the CatWalk test (Figure 1(b)), the %TIPPI decreased from 50.1 ± 1.3 on
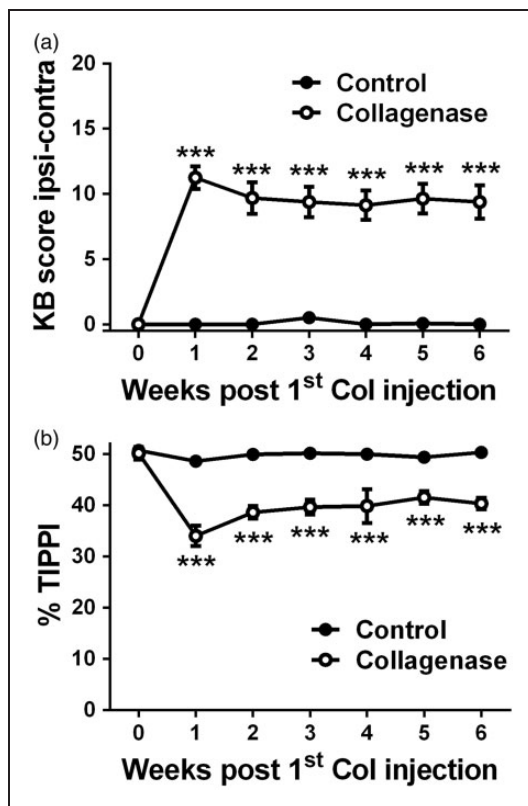

Figure 1. Nociceptive behaviour. Nociception associated with movement and loading on the joint was evaluated by the Knee-Bend (a) and CatWalk (b) tests in saline-injected control and collagenase-injected OA animals. Knee-Bend score (a) is presented as the difference between ipsilateral and contralateral scores. CatWalk data (b) are expressed as the percentage of total ipsilateral paw print intensity (%TIPPI). Mean $\pm$ SEM, two-way ANOVA followed by Bonferroni post-hoc test for comparisons between groups at each time point. ***$p < 0.001$, comparisons between the control and the collagenase group.

day 0 to 34.0 ± 2.0 at week 1 ($p < 0.001$), when the lowest values were observed. The %TIPPI remained significantly lower from control animals during the whole experimental period (40.3 ± 1.1, $p < 0.001$).

Glial activation in the DRG

SGC activation in the DRG was assessed through the expression of GFAP both by immunofluorescence and WB analysis. For GPAP immunolabelling (Figure 2(a) and (b)), the percentage of GFAP-encircled neurons six weeks after OA induction increased from $5.6 \pm 1.4\%$ in controls to $21.9 \pm 3.2\%$ in collagenase-injected animals ($p < 0.01$, Figure 2(c)). WB analysis in the DRG innervating the knee joint (Figure 2(d)) confirmed the increased expression of GFAP protein in the ipsilateral ganglia of collagenase-injected animals at six weeks of OA development (Figure 2(d)). WB quantification showed that although there is a similar expression of GFAP in the ipsilateral and contralateral DRG of control animals, with an ipsilateral/contralateral ratio of 1.02 ± 0.07, the ipsilateral/contralateral ratio in collagenase-injected animals significantly increases to 1.50 ± 0.18 ($p < 0.01$, Figure 2(d)).

In order to determine if GFAP was preferentially expressed in SGCs surrounding injured neurons, double immunolabelling for GFAP and ATF-3 (Figure 3(a) and (b)) was performed for the six weeks of OA group. While in control animals $7.5 \pm 5.0\%$ of ATF-3-positive neurons were encircled by GFAP-labelled SGCs, in collagenase-injected animals this percentage increased to $35.0 \pm 4.0\%$ ($p < 0.01$, Figure 3(c)).

Glial activation in the SC

The activation of astrocytes and microglia in the SC was analysed through the expression of GFAP (Figure 4) and IBA-1 (Figure 5), respectively. Immunohistochemistry (Figure 4(a) to (f)) followed by densitometric (Figure 4(g)) analysis was used to evaluate expression changes specifically in laminae I–III of the spinal dorsal horn. There was a small but significant increase in the ipsilateral/contralateral ratio of GFAP expression in the dorsal horn of the L3–L5 segments of the SC of collagenase-injected rats; control animals (Figure 4(c) and (d)) had a ratio of 1.01 ± 0.01, whereas OA rats (Figure 4(e) and (f)) had a ratio of 1.12 ± 0.03 ($p < 0.01$, Figure 4(g)). WB analysis included the whole ipsilateral and contralateral hemisegments of the SC and showed that the ipsilateral/contralateral ratio of GFAP expression in the L3–L5 hemisegments increased from 0.97 ± 0.07 to 1.18 ± 0.10, although this difference was not significant (Figure 4(h)). For IBA-1 expression in the SC (Figure 5(a) to (f)), there were no significant differences in the immunolabelling in laminae I–III (Figure 5(g)),
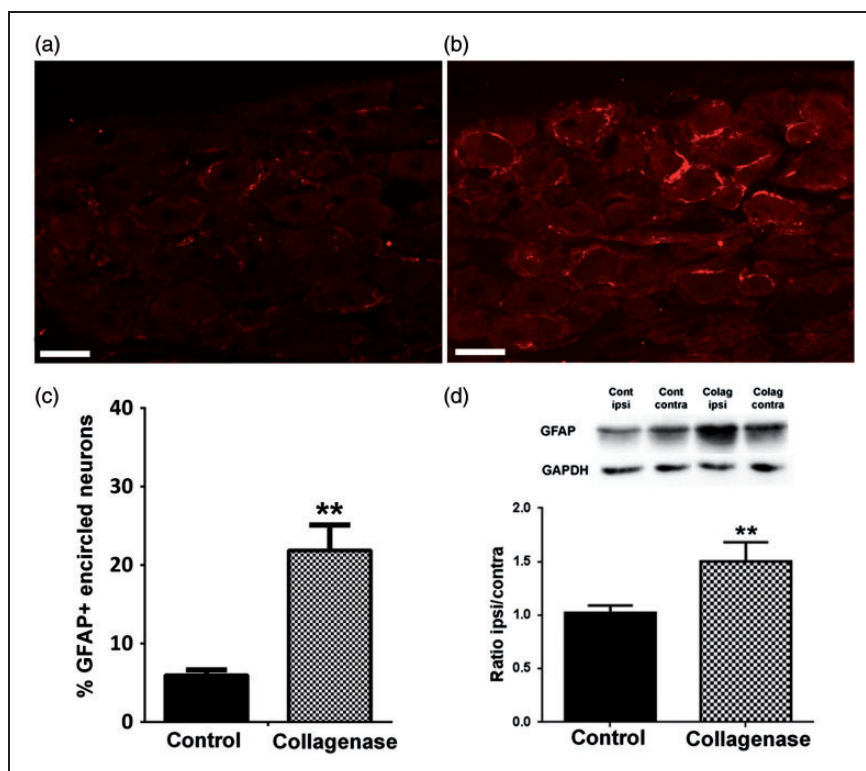
Figure 2. GFAP expression in the DRG. Representative images of GFAP labelling in SGCs of L4 DRG, six weeks after the first saline (a) or collagenase (b) injection; Scale bar: 50 μm. (c) Immunofluorescence analysis of GFAP expression in L3, L4 and L5 ipsilateral DRG of saline- and collagenase-injected rats, six weeks after injection; GFAP expression significantly increased at six weeks of OA. Data are presented as the percentage of GFAP-encircled neurons in L3, L4 and L5 DRG. (d) Western Blot analysis of GFAP levels in L3–L5 DRG of control and collagenase-injected rats, six weeks after injection. Results are presented as the ipsilateral/contralateral ratio of GFAP levels (GFAP/GAPDH values). Mean ± SEM. Mann–Whitney test, $**p < 0.01$, for comparisons between control and collagenase-injected animals.

with an ipsilateral/contralateral ratio of 1.00 ± 0.03 in control animals (Figure 5(c) and (d)) and of 1.08 ± 0.03 in OA rats (Figure 5(e) and (f)). However, when analysing by WB the L3–L5 hemisegments, there was a significant increase in IBA-1 expression from an ipsilateral/contralateral ratio of 1.00 ± 0.06 in control animals to 1.48 ± 0.15 in OA animals ($p < 0.05$, Figure 5(h)).

Inhibition of glial activation

The effect of fluorocitrate on movement-induced nociception in collagenase-injected animals with six weeks of OA development was also evaluated (Figure 6). All animals showed significant nociceptive behaviour before drug or vehicle administration ($t = 0$ h, baseline). While intrathecal vehicle administration had no effect, intrathecal fluorocitrate administration decreased OA-induced nociception in both tests (Figure 6(a) and (b)). In the Knee-Bend test (Figure 6(a)), rats receiving fluorocitrate showed a significant decrease from 1 h onwards, from a baseline value of 10.1 ± 1.3 to a value of 4.8 ± 0.9 at 2 h (P < 0.001), when peak effect was observed, reverting thereafter. In the CatWalk test (Figure 6(b)), the

observed decrease in OA-induced nociception was also significant 2 and 3 h after fluorocitrate administration, with the %TIPPI increasing from a baseline value of 33.8 ± 1.3 to 43.4 ± 2.1 at 3 h ($p < 0.01$), when peak effect was observed.

Discussion

Glial activation has been increasingly regarded has a key player in the modulation of nociception. Therefore, this study aimed at determining if glial activation could also contribute to the mechanisms of nociception in knee OA induced by i.a. injection of collagenase in rats. Overall, we observed that there is indeed an increased glial activation both in the DRG and in the SC of OA rats. Furthermore, we observed that the inhibition of glial activation can decrease the nociceptive behaviours associated with movement and loading on OA joints, which mimic patients' major complaints.[42]

In previous studies using the collagenase model of OA, we showed an overexpression of the neuronal injury markers ATF-3 and NPY in the DRG of OA animals.[1] After six weeks of OA progression, there was
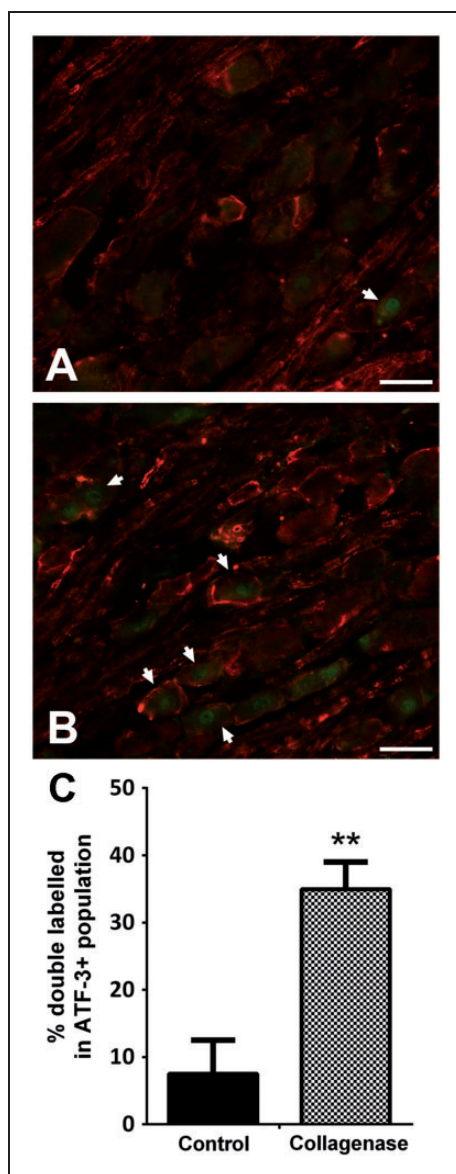
Figure 3. ATF-3 and GFAP double labelling. Representative images of double immunofluorescence labelling for ATF-3 and GFAP in L4 ipsilateral DRG of saline-injected (a) and collagenase-injected (b) rats, six weeks after injection. Scale bar: 50 μm. (c) The percentage of GFAP-encircled neurons within the ATF-3 positive population increased in collagenase-injected animals in comparison with control animals. Mean ± SEM. Mann–Whitney test; **$p < 0.01$.

extensive articular degeneration that correlated with the nociceptive behaviour.[5] The degree of articular degeneration also correlated with the upregulation of neuronal injury markers,[1] as well as with a progressive decrease in fluorogold (FG) backlabelling from collagenase-injected joints,[1] which may be attributed to injury of nerve endings interfering with FG uptake. These findings, along with the observation that gabapentin, effective in neuropathic pain, could reverse the nociceptive behaviour in the collagenase model,[1] strongly pointed to the occurrence of PNI and to a potential neuropathic component in the mechanisms of nociception associated to OA in this model.

Given the known effect of PNI on the activation state of glia in both the PNS and CNS,[6–9] we evaluated whether the progression of collagenase-induced OA could have a similar effect on glial activation at six weeks, when all the major changes had been detected and neuropathy correlated with nociception. We observed a significant increase in GFAP expression, a marker of SGC activation, in the DRG of OA animals after six weeks of OA progression, as shown both by WB and immunofluorescence. Aiming at establishing a link between neuronal injury and SGC activation, we evaluated if SGCs overexpressing GFAP were preferentially located around injured neurons identified by ATF-3 expression.[30] A significant increase in the proportion of GFAP-encircled neurons within the ATF-3-expressing population was indeed found in collagenase-injected animals, with around 35% of ATF-3-positive neurons being surrounded by activated SGCs. Nevertheless, increased GFAP expression was also observed around neurons that did not have upregulated ATF-3 expression. Likewise, studies in chronic constriction injury of the infraorbital nerve have shown that, although SGC activation occurs preferentially around trigeminal ganglia neurons expressing ATF-3, GFAP expression associated with SGC activation is not restricted to those neurons.[43] SGC activation leads to an increase in the number of gap junctions, which are known to promote communication between adjacent SGCs enveloping neighbouring neurons and even contribute to nociception.[44–46] Furthermore, there are numerous molecules released by neurons whose receptors are found in SGCs, revealing potential pathways of neuroglial crosstalk and of SGC activation.[47,48] Indeed, SGCs have been increasingly regarded as more than just supporting cells in the DRG,[15] and evidence for a role of SGCs in direct neurochemical transmission between neighbouring neurons has emerged recently.[49,50] Functional changes induced by neuronal injury in collagenase-induced OA may therefore be communicated to neighbouring neurons and SGCs, leading to the activation of SGCs around uninjured neurons.

Glial activation in the CNS also plays an important role in neuropathic pain.[6–9] Here, we show that collagenase-injected rats have increased IBA-1 expression at six weeks in the ipsilateral hemisegment of the SC analysed by WB; immunohistochemical analysis of laminae I–III of the spinal dorsal horn showed no significant changes. A different pattern was observed for GFAP expression, which was shown to be increased in laminae I-III of the ipsilateral spinal dorsal horn while WB analysis of the whole ipsilateral hemisegment showed no significant changes. In models of neuropathic pain, microglial
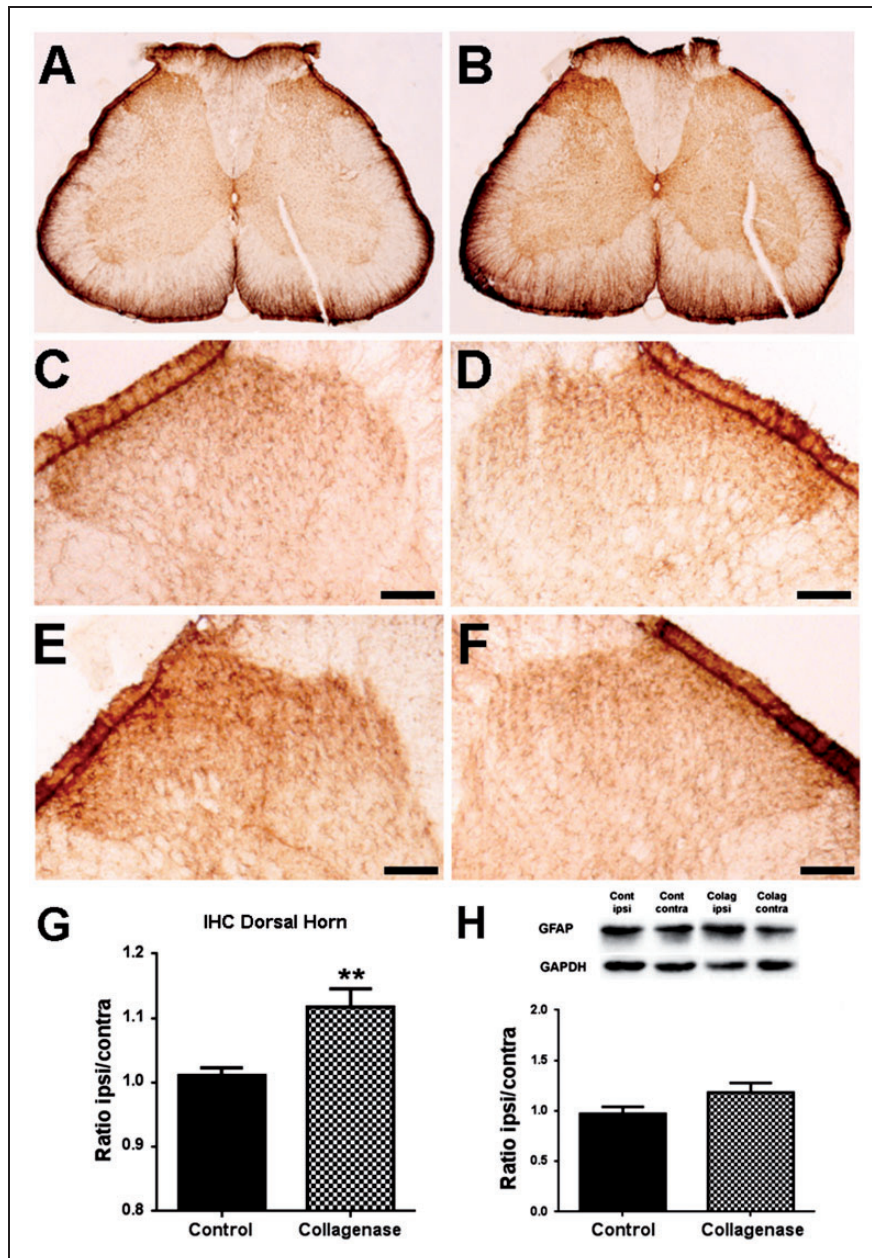
Figure 4. GFAP expression in the spinal cord. Representative images of GFAP labelling in the SC, six weeks after the first saline (a) or collagenase (b) injection. Representative images of GFAP labelling in the ipsilateral (c, e) and contralateral (d, f) dorsal horn, six weeks after the first saline (c, d) or collagenase (e, f) injection; Scale bar: 50 μm. (g) Densitometric quantification of GFAP labelling in laminae I-III of the dorsal horn of control and collagenase-injected rats six weeks after injection, presented as the ipsilateral/contralateral ratio. (h) Quantitative WB analysis of GFAP expression in the spinal cord of control and collagenase-injected rats six weeks after injection, presented as the ipsilateral/contralateral ratio of GFAP levels (GFAP/GAPDH). Mean ± SEM. Mann–Whitney test; $**p < 0.01$.

activation seems to occur preferentially during the early phases of disease development.[9,51] Neuronal injury induces a set of progressive alterations in spinal microglia, with early morphological changes[52] being followed by proliferation in the ipsilateral spinal dorsal horn[53] associated with increased secretion of cytokines, chemokines and neurotrophic factors that alter neuronal excitability. This microglia–neuron communication is increasingly recognized as a key contributor to neuropathic pain.[54] Thakur et al.[3] have previously reported increased spinal microglial activation in both the ipsilateral dorsal and ventral horns in the MIA model of OA. Other studies also showed increased microglial activation specifically in the ipsilateral dorsal horn. The main variable between these studies was the temporal profile of microglial activation, with dorsal horn changes peaking
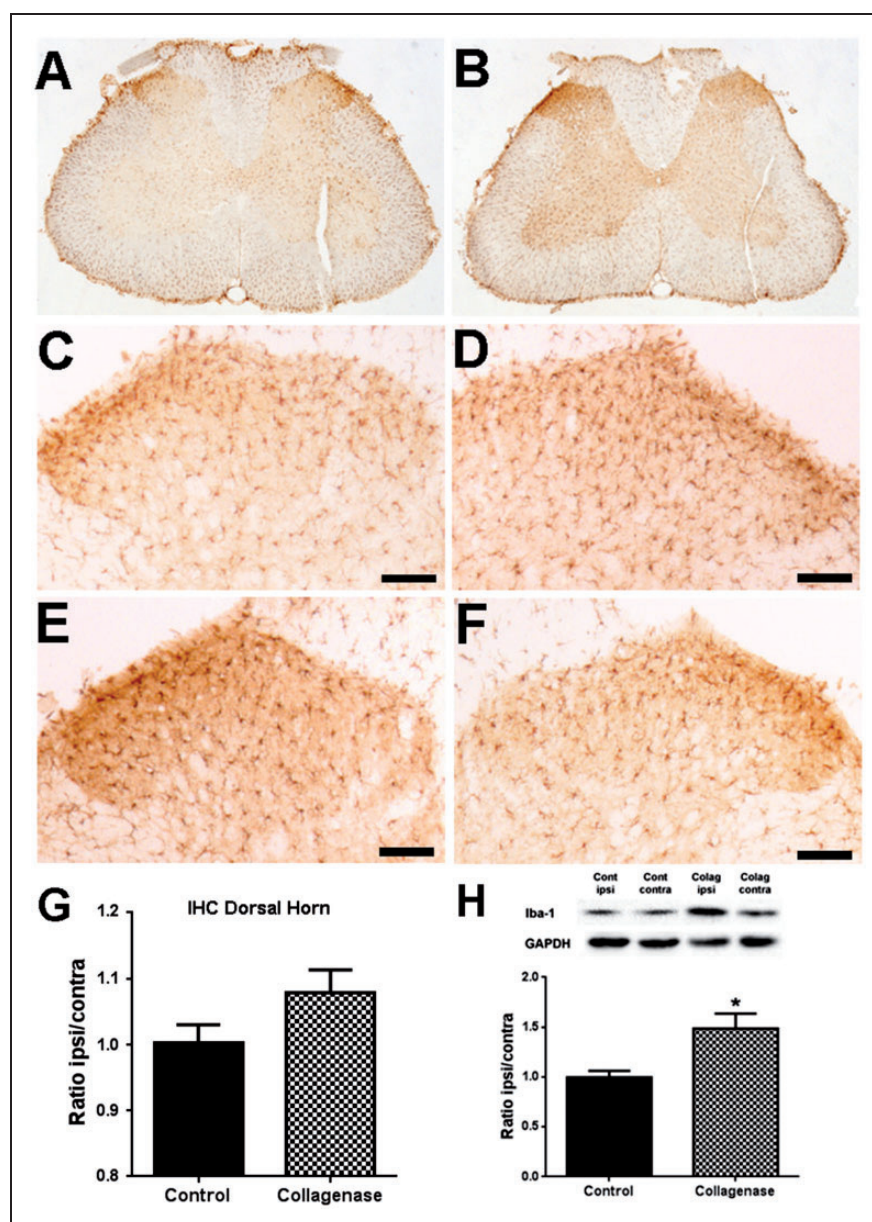
Figure 5. Iba-1 expression in the Spinal Cord. Representative images of Iba-1 labelling in the SC, six weeks after the first saline (a) or collagenase (b) injection. Representative images of Iba-1 labelling in the ipsilateral (c, e) and contralateral (d, f) dorsal horn, six weeks after the first saline (c, d) or collagenase (e, f) injection; Scale bar: 50 µm. (g) Densitometric quantification of Iba-1 labelling in laminae I–III of the dorsal horn of control and collagenase-injected rats six weeks after injection, presented as the ipsilateral/contralateral ratio. (h) Quantitative WB analysis of Iba-1 expression in the spinal cord of control and collagenase-injected rats six weeks after injection, presented as the ipsilateral/contralateral ratio of Iba-1 levels (Iba-1/GAPDH). Mean ± SEM. Mann–Whitney test; **$p < 0.01$.

either 7[3] or 14 days[55] after OA induction and decreasing thereafter, or being maintained in later stages of OA, after 28 days[56] or 6 weeks.[57] Although it is possible that dorsal horn specific changes occur at earlier time points of collagenase-induced OA development, at six weeks, significant microglial activation, as evaluated by IBA-1 increased expression, was observed in the whole ipsilateral spinal hemisegment. Microglial cells have a characteristic low threshold for reactivity and are known to respond to a wide range of stimuli.[58] It is possible that initial changes occurring in the spinal dorsal horn may extend to other areas of the SC through intercellular communication, inducing the widespread activation observed in this model. Although it would be interesting to assess if microglial activation occurs earlier in OA progression, this was not our goal in this study since we focused this analysis on a time point when OA-like changes are already fully developed.[5]
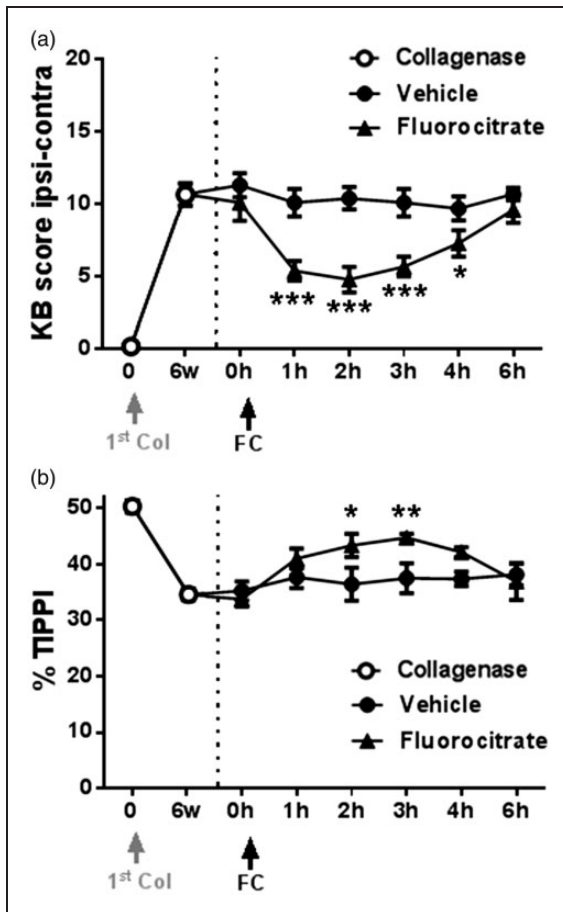
Figure 6. Fluorocitrate administration. The effect of fluorocitrate administration (30 μL, 0.1 nM, intrathecal) on movement- and loading-induced nociception was assessed by the Knee-Bend (a) and the CatWalk (b) tests six weeks after injection of collagenase. Nociception was assessed on day 0, before the first collagenase injection, and before fluorocitrate administration for determination of baseline values (open circles); the effect of fluorocitrate or vehicle was determined 1, 2, 3, 4 and 6 h after administration (filled symbols). Mean ± SEM. Repeated measures ANOVA followed by Dunnett's post-hoc test; *$p < 0.05$, **$p < 0.01$, ***$p < 0.001$.

Astrocyte activation associated with neuropathic pain has been shown to start at later stages after injury and to be long lasting.[9,51] Interestingly, a similar pattern has been observed in animal models of OA. Indeed, in the MIA model, no significant changes in GFAP expression in the SC have been observed until 14 days of disease progression,[3] but an increased GFAP expression in the dorsal horn at later time points ranging from three to six weeks has been reported.[55,57] Likewise, we observed a significant increase in GFAP expression in the ipsilateral dorsal horn. This preferential increase of GFAP in laminae I–III may be associated with an increased activity of nociceptive neurons leading to an augmented local release of glutamate. Research has shown that an increase in extracellular glutamate causes the activation

of astrocytes mediated by the type II metabotropic glutamate receptors mGluR 2/3, which are expressed in astrocytes.[59] The extracellular increase in glutamate also triggers the production of the glial high-affinity glutamate transporter GLAST. Since GFAP acts to anchor GLAST at the plasma membrane of glial cells,[60] an increase in extracellular glutamate can induce an increase in GFAP expression. A similar mechanism may also account for the increased expression of GFAP in SGCs.

Glial and immune cells activation has been gaining ground as a potential pharmacological target for controlling chronic pain. A number of drugs have been shown to suppress the development of neuropathic pain by reducing glial activation, and consequently decreasing the secretion of numerous cytokines known to contribute to the development and maintenance of neuropathic pain.[61] One such drug is fluorocitrate, which has been shown to attenuate nociception in different models of neuropathy.[61] Fluorocitrate acts by selectively inhibiting glial cell metabolism,[28,29] with no specific selectivity for different glial cells types, transiently inactivating microglia, astrocytes and SGCs. Therefore, as activation of all those glial cells types had been observed, we evaluated the effect of an intrathecal administration of fluorocitrate in movement- and loading-induced nociception to determine if glial activation could contribute to the nociceptive behaviour in the collagenase model of OA. We observed that fluorocitrate significantly reduced movement- and loading-induced nociception evaluated by the Knee-Bend and CatWalk tests. This is in line with studies in the MIA OA model, in which the glial activation inhibitor minocycline significantly attenuated the nociceptive behaviour.[55] These results suggest a role for glial cells in the development of nociceptive behaviours in the collagenase model of OA, and place these cells as pharmacological targets worth pursuing.

Altogether, the data here presented show that when OA is fully developed, with extensive articular damage associated with movement and loading-induced nociception, there is activation of glial cells both in the DRG and in the SC, and their inactivation can significantly reduce OA-associated nociception. These results therefore suggest that glial activation associated with PNI may play a role in nociception associated with OA.

Declaration of Conflicting Interests

Funding

References

1. Adães S, Ferreira-Gomes J, Mendonça M, et al. Injury of primary afferent neurons may contribute to osteoarthritis induced pain: an experimental study using the collagenase model in rats. *Osteoarthr Cartil* 2015; 23: 914–924.

2. Ferreira-Gomes J, Adães S, Sousa RM, et al. Dose-dependent expression of neuronal injury markers during experimental osteoarthritis induced by monoiodoacetate in the rat. *Mol Pain* 2012; 8: 50.

3. Thakur M, Rahman W, Hobbs C, et al. Characterisation of a peripheral neuropathic component of the rat mono-iodoacetate model of osteoarthritis. *PLoS One* 2012; 7: e33730.

4. Thakur M, Dickenson AH and Baron R. Osteoarthritis pain: nociceptive or neuropathic? *Nat Rev Rheumatol* 2014; 10: 374–380.

5. Adães S, Mendonça M, Santos TN, et al. Intra-articular injection of collagenase in the knee of rats as an alternative model to study nociception associated with osteoarthritis. *Arthritis Res Ther* 2014; 16: R10.

6. Scholz J and Woolf CJ. The neuropathic pain triad: neurons, immune cells and glia. *Nat Neurosci* 2007; 10: 1361–1368.

7. Cao H and Zhang YQ. Spinal glial activation contributes to pathological pain states. *Neurosci Biobehav Rev* 2008; 32: 972–983.

8. Suter MR, Wen Y-R, Decosterd I, et al. Do glial cells control pain? *Neuron Glia Biol* 2007; 3: 255–268.

9. Gosselin R-D, Suter MR, Ji R-R, et al. Glial cells and chronic pain. *Neuroscientist* 2010; 16: 519–531.

10. Pannese E. The structure of the perineuronal sheath of satellite glial cells (SGCs) in sensory ganglia. *Neuron Glia Biol* 2010; 6: 3–10.

11. Takeda M, Takahashi M and Matsumoto S. Contribution of the activation of satellite glia in sensory ganglia to pathological pain. *Neurosci Biobehav Rev* 2009; 33: 784–792.

12. Liu F-Y, Sun Y-N, Wang F-T, et al. Activation of satellite glial cells in lumbar dorsal root ganglia contributes to neuropathic pain after spinal nerve ligation. *Brain Res* 2012; 1427: 65–77.

13. Kim D-S, Figueroa KW, Li K-W, et al. Profiling of dynamically changed gene expression in dorsal root ganglia post peripheral nerve injury and a critical role of injury-induced glial fibrillary acidic protein in maintenance of pain behaviors [corrected]. *Pain* 2009; 143: 114–122.

14. Hanani M. Satellite glial cells in sensory ganglia: from form to function. *Brain Res Brain Res Rev* 2005; 48: 457–476.

15. Ohara PT, Vit J-P, Bhargava A, et al. Gliopathic pain: when satellite glial cells go bad. *Neuroscientist* 2009; 15: 450–463.

16. Zhang H, Mei X, Zhang P, et al. Altered functional properties of satellite glial cells in compressed spinal ganglia. *Glia* 2009; 57: 1588–1599.

17. Xie W, Strong JA and Zhang J-M. Early blockade of injured primary sensory afferents reduces glial cell activation in two rat neuropathic pain models. *Neuroscience* 2009; 160: 847–857.

18. Xu M, Aita M and Chavkin C. Partial infraorbital nerve ligation as a model of trigeminal nerve injury in the mouse: behavioral, neural, and glial reactions. *J Pain* 2008; 9: 1036–1048.

19. Dubový P, Klusáková I, Svízenská I, et al. Satellite glial cells express IL-6 and corresponding signal-transducing receptors in the dorsal root ganglia of rat neuropathic pain model. *Neuron Glia Biol* 2010; 6: 73–83.

20. Woodham P, Anderson PN, Nadim W, et al. Satellite cells surrounding axotomised rat dorsal root ganglion cells increase expression of a GFAP-like protein. *Neurosci Lett* 1989; 98: 8–12.

21. Milligan ED and Watkins LR. Pathological and protective roles of glia in chronic pain. *Nat Rev Neurosci* 2009; 10: 23–36.

22. Takeda M, Tanimoto T, Kadoi J, et al. Enhanced excitability of nociceptive trigeminal ganglion neurons by satellite glial cytokine following peripheral inflammation. *Pain* 2007; 129: 155–166.

23. Allen NJ and Barres BA. Neuroscience: Glia – more than just brain glue. *Nature* 2009; 457: 675–677.

24. Markiewicz I and Lukomska B. The role of astrocytes in the physiology and pathology of the central nervous system. *Acta Neurobiol Exp (Wars)* 2006; 66: 343–358.

25. Miller G. Neuroscience. The dark side of glia. *Science* 2005; 308: 778–781.

26. Miller TR, Wetter JB, Jarvis MF, et al. Spinal microglial activation in rat models of neuropathic and osteoarthritic pain: an autoradiographic study using [3H]PK11195. *Eur J Pain* 2013; 17: 692–703.

27. Zhang SC, Goetz BD and Duncan ID. Suppression of activated microglia promotes survival and function of transplanted oligodendroglial progenitors. *Glia* 2003; 41: 191–198.

28. Hassel B, Paulsen RE, Johnsen A, et al. Selective inhibition of glial cell metabolism in vivo by fluorocitrate. *Brain Res* 1992; 576: 120–124.

29. Paulsen RE, Contestabile A, Villani L, et al. An in vivo model for studying function of brain tissue temporarily devoid of glial cell metabolism: the use of fluorocitrate. *J Neurochem* 1987; 48: 1377–1385.

30. Tsujino H, Kondo E, Fukuoka T, et al. Activating transcription factor 3 (ATF3) induction by axotomy in sensory and motoneurons: A novel neuronal marker of nerve injury. *Mol Cell Neurosci* 2000; 15: 170–182.

31. Raghavendra V, Tanga F and DeLeo JA. Inhibition of microglial activation attenuates the development but not existing hypersensitivity in a rat model of neuropathy. *J Pharmacol Exp Ther* 2003; 306: 624–630.

32. Zimmermann M. Ethical guidelines for investigations of experimental pain in conscious animals. *Pain* 1983; 16: 109–110.

33. Kikuchi T, Sakuta T and Yamaguchi T. Intra-articular injection of collagenase induces experimental osteoarthritis in mature rabbits. *Osteoarthritis Cartilage* 1998; 6: 177–186.

34. Ferreira-Gomes J, Adães S and Castro-Lopes JM. Assessment of movement-evoked pain in osteoarthritis by the knee-bend and CatWalk tests: a clinically relevant study. *J Pain* 2008; 9: 945–954.

35. Lu W and Haber SN. In situ hybridization histochemistry: A new method for processing material stored for several years. *Brain Res* 1992; 578: 155–160.

36. Nascimento DSM, Castro-Lopes JM and Neto FLM. Satellite glial cells surrounding primary afferent neurons are activated and proliferate during monoarthritis in rats: is there a role for ATF3? *PLoS One* 2014; 9: e108152.

37. Cruz CD, Neto FL, Castro-Lopes J, et al. Inhibition of ERK phosphorylation decreases nociceptive behaviour in monoarthritic rats. *Pain* 2005; 116: 411–419.

38. Paxinos G and Watson C. *The rat brain in stereotaxic coordinates*, 2nd ed. Orlando, FL: Academic Press, 1986.

39. Sun S, Chen WL, Wang PF, et al. Disruption of glial function enhances electroacupuncture analgesia in arthritic rats. *Exp Neurol* 2006; 198: 294–302.

40. Ossipov MH, Suarez LJ and Spaulding TC. A comparison of the antinociceptive and behavioral effects of intrathecally administered opiates, alpha-2-adrenergic agonists, and local anesthetics in mice and rats. *Anesth Analg* 1988; 67: 616–624.

41. De la Calle JL and Paíno CL. A procedure for direct lumbar puncture in rats. *Brain Res Bull* 2002; 59: 245–250.

42. Creamer P, Lethbridge-Cejku M and Hochberg MC. Where does it hurt? Pain localization in osteoarthritis of the knee. *Osteoarthritis Cartilage* 1998; 6: 318–323.

43. Donegan M, Kernisant M, Cua C, et al. Satellite glial cell proliferation in the trigeminal ganglia after chronic constriction injury of the infraorbital nerve. *Glia* 2013; 61: 2000–2008.

44. Hanani M, Caspi A and Belzer V. Peripheral inflammation augments gap junction-mediated coupling among satellite glial cells in mouse sympathetic ganglia. *Neuron Glia Biol* 2010; 6: 85–89.

45. Huang T-Y, Belzer V and Hanani M. Gap junctions in dorsal root ganglia: possible contribution to visceral pain. *Eur J Pain* 2010; 14: 49.e1–e11.

46. Hanani M, Huang T, Cherkas P, et al. Glial cell plasticity in sensory ganglia induced by nerve damage. *Neuroscience* 2002; 114: 279–283.

47. Fields RD and Burnstock G. Purinergic signalling in neuron-glia interactions. *Nat Rev Neurosci* 2006; 7: 423–436.

48. Kung L-H, Gong K, Adedoyin M, et al. Evidence for glutamate as a neuroglial transmitter within sensory ganglia. *PLoS One* 2013; 8: e68312.

49. Rozanski GM, Li Q and Stanley EF. Transglial transmission at the dorsal root ganglion sandwich synapse: glial cell to postsynaptic neuron communication. *Eur J Neurosci* 2013; 37: 1221–1228.

50. Rozanski GM, Kim H, Li Q, et al. Slow chemical transmission between dorsal root ganglion neuron somata. *Eur J Neurosci* 2012; 36: 3314–3321.

51. Hald A, Nedergaard S, Hansen RR, et al. Differential activation of spinal cord glial cells in murine models of neuropathic and cancer pain. *Eur J Pain* 2009; 13: 138–145.

52. Eriksson NP, Persson JKE, Svensson M, et al. A quantitative analysis of the microglial cell reaction in central primary sensory projection territories following peripheral nerve injury in the adult rat. *Exp Brain Res* 1993; 96: 19–27.

53. Calvo M and Bennett DLH. The mechanisms of microgliosis and pain following peripheral nerve injury. *Exp Neurol* 2012; 234: 271–282.

54. Tsuda M, Masuda T, Tozaki-Saitoh H, et al. Microglial regulation of neuropathic pain. *J Pharmacol Sci* 2013; 121: 89–94.

55. Sagar DR, Burston JJ, Hathway GJ, et al. The contribution of spinal glial cells to chronic pain behaviour in the monosodium iodoacetate model of osteoarthritic pain. *Mol Pain* 2011; 7: 88.

56. Orita S, Ishikawa T, Miyagi M, et al. Pain-related sensory innervation in monoiodoacetate-induced osteoarthritis in rat knees that gradually develops neuronal injury in addition to inflammatory pain. *BMC Musculoskelet Disord* 2011; 12: 134.

57. Yu D, Liu F, Liu M, et al. The inhibition of subchondral bone lesions significantly reversed the weight-bearing deficit and the overexpression of CGRP in DRG Neurons, GFAP and Iba-1 in the spinal dorsal horn in the monosodium iodoacetate induced model of osteoarthritis pain. *PLoS One* 2013; 8: e77824.

58. Trang T, Beggs S and Salter MW. ATP receptors gate microglia signaling in neuropathic pain. *Exp Neurol* 2012; 234: 354–361.

59. Romão LF, De Sousa VO, Neto VM, et al. Glutamate activates GFAP gene promoter from cultured astrocytes through TGF-β1 pathways. *J Neurochem* 2008; 106: 746–756.

60. Sullivan SM, Lee A, Björkman ST, et al. Cytoskeletal anchoring of GLAST determines susceptibility to brain damage: An identified role for GFAP. *J Biol Chem* 2007; 282: 29414–29423.

61. Mika J, Zychowska M, Popiolek-Barczyk K, et al. Importance of glial activation in neuropathic pain. *Eur J Pharmacol* 2013; 716: 106–119.